Adv Polym Sci (2021) 287: 75–104
https://doi.org/10.1007/12_2021_88

Published online: 9 July 2021

# Synthesis and Modification Strategies of Chitosan and Its Interaction with Metal Ions


**Muthu Prabhu Subbaiah and Meenakshi Sankaran**

## Contents



**Abstract** Chitosan is one of the most important and widely available biomaterials produced by nature for remediation of its resources. It is obtained by deacetylation of chitin extracted from marine waste materials and highly useful to adsorb the toxic ions existing in the water body as it has a large number of active functionalities of hydroxyl and amine groups. The chitosan has several advantages including low cost, bio-degradable, and bio-compatibility over other chemically synthesized materials in the laboratory. Different chitosan-based materials have been identified and tested in the removal of toxic anions, especially, metals, metalloids, dyes, hydrocarbons,

M. P. Subbaiah
Department of Chemistry, Gandhigram Rural Institute – Deemed to be University, Dindigul, Tamil Nadu, India

Department of Earth Resources and Environmental Engineering, Hanyang University, Seoul, South Korea

M. Sankaran (✉)
Department of Chemistry, Gandhigram Rural Institute – Deemed to be University, Dindigul, Tamil Nadu, India

organic pesticides, etc. In this review, we focused on the functionalized forms of chitosan with metal ions and their adsorption on toxic ions, such as fluoride, phosphate, nitrate, and arsenic from waters using batch experiments. Also, it intensively focused on the synthetic methods, feasibility, and the regeneration/reusability of the materials. The results of this review indicated that the metal-loaded chitosan-based composite materials have shown much higher efficiency than the raw forms of chitosan and metal/metal oxides or hydroxides due to the synergistic interaction and the affinity of the materials. In particular, the mechanism of interactions of toxic ions and the metal ions present in the composites was thoroughly reviewed using analytical and the experimental data that existed in the literature. The reported adsorption densities, collected by recently reported materials, and the selectivity test results were much higher than those of other bio-based materials and inorganic nanocomposites. This review critically discussed the real-water analysis, cost-effectiveness of the reported materials. Importantly, the clean-up and the disposal methods for the pollutant sorbed materials and other areas requiring further research were addressed.

**Keywords** Adsorption · Arsenic · Chitosan · Fluoride · Nitrate · Phosphate

## 1 Introduction

A large amount of biomass waste is discarded into the environment without pretreatment. For example, shrimp shell waste is generated in huge quantities from the shrimp industries throughout the world, and it is primarily disposed of into the sea, resulting in intense environmental pollution [1]. India is a major producer of shrimp, which is more than 1,00,000 tons of shrimp bio-waste generated annually and only an insignificant amount of that bio-waste is utilized for the extraction of chitin while the rest is discarded. According to the report in 2012, a total of 250 chitinolytic bacteria from 68 different marine samples were screened by employment enrichment method which utilized native chitin as the sole carbon source. The shrimp shell waste is utilized for the production of natural biopolymers like chitin, chitosan, N-acetyl glucosamine, chitooligosaccharide, other essential amino acids, etc. [2]. Chitin was prepared by a two-step extraction method from shrimp shells using citric acids and deep eutectic solvents. The acids could effectively remove some minerals and proteins followed by deep eutectic solvents with the assistance of microwave and the deproteinization efficiency was more than 88% [3]. It is a linear amino polysaccharide comprised of β-(1,4)-2-deoxy-2-acetamido-D-glucopyranose structure and the deacetylated form of chitin is known as chitosan, i.e., β-(1,4)-2-deoxy-2-amino-D-glucopyranose using NaOH and the chitin with a degree of deacetylation of above 70% is considered as chitosan. Chitosan is insoluble in water but soluble in acetic acid solvents below pH 6. Monoprotic acids such as formic, acetic, hydrochloric, and lactic acids are used for dissolving chitosan, and mostly 1% acetic acid solution used to dissolve chitosan. But it does not dissolve in

diprotic and polyprotic acids such as sulfuric and phosphoric acids and it has poor stability over pH 7 due to precipitation/gelation that takes place in the alkali pH range. Chitosan solution forms a poly–ion complex with anionic hydrocolloid to produce a gel.

## 2 Chemistry of Chitosan

### *2.1 Covalent Functionalization of Chitosan Without Metal Ions*

Chitosan is used to modify chemically to change its structure and properties to meet the requirements of specific applications. The free amine groups are strongly reactive and can be easily modified chemically or physically. One simple modification of chitosan is protonation. Besides, the protonation of amine groups in acidic solutions gives the chitosan a cationic behavior and consequently the potential for attracting the negatively charged species [4]. The protonated form of chitosan is useful to attract negatively charged species like fluoride, chromate ions, and anionic dyes from water through electrostatic interactions [5, 6]. Initially, Viswanathan and Meenaksi have developed protonated chitosan beads (PCB) for fluoride removal from water, in which they found a maximum uptake of fluoride ions of 1664 mg/kg [5], then for copper uptake densities on chemically functionalized chitosan beads were 52, 86, and 126 mg/g for protonated chitosan beads, carboxylated chitosan beads, and grafted chitosan beads, respectively [7] using the same adsorbent was Pokhrel et al. have reported a review article on the chemical functionalization of chitosan and their applications, in which the chemical and physical functionalization of chitosan without altering the degrees of solubilization [8]. Amine groups were responsible to modify chemically with other functional groups rather than hydroxyl groups due to their basic nature for various applications. In 2015, Macquarrie and Hardy have reviewed the chemically bonded groups on chitosan without metal ions for catalysis inorganic transformations [9]. Recently, Mincke et al. [10] have developed chemically functionalized chitosan adsorbents for selective recovery of palladium and platinum groups from acidic aqueous solutions. In this article, the authors have used various functionalities, viz. 1,10-phenanthroline-2,9-dicarbaldehyde (Ch-PDC), [2,2′-bipyridine]-5,5′-dicarbaldehyde (Ch-BPDC), and glutaraldehyde cross-linked chitosan grafted with 8-hydroxyquinoline-2-carbaldehyde (Ch-GA-HQC) for selective recovery of Pd(II) and Pt(IV) metal ions from waters. The obtained maximum adsorption densities based on Langmuir isotherm were 340.3 and 203.9 mg/g for Pb(II) and Pt(IV), respectively, on (Ch-GA-HQC). The sorption mechanism established by external mass transfer is followed by the intra-particle diffusion process and chemisorption [10]. Likewise, a 3D sponge of 11-mercaptoundecanoic acid-functionalized chitosan (MUA) as an effective adsorbent for methyl orange adsorption was also used for antibiotic-free antibacterial activity. The maximum uptake of methyl orange was 388 mg/g, which is much higher

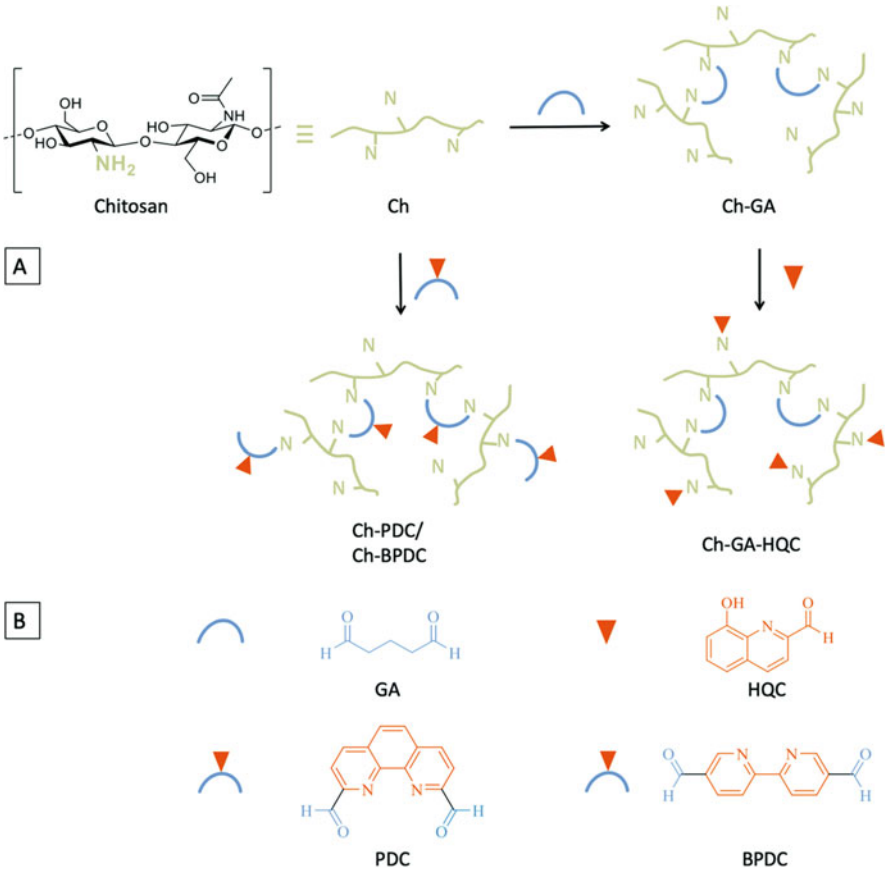


**Fig. 1** Schematic overview of the (**a**) synthesis of Ch-PDC, Ch-BPDC, and Ch-GA-HQC and (**b**) the chelating and cross-linking compounds. The figure was adapted with permission from Ref. [10]

adsorption densities compared to many chitosan-based adsorbents in the literature [11]. Interestingly, to improve the adsorption efficiencies of the metals from water, the chitosan moiety was functionalized with more amine groups which tend to be complexed with metal ions easily. Zarghami et al. have developed polyamidoamine (PAMAM)-grafted dendrimer through a divergent growth approach, in which the Pb (II) ions were successful [12]. Moreover, the chemical functionalization of chitosan using different strategies was proposed by Ji et al. for drug delivery systems in detail [13]. Padmaja group has delivered a superabsorbent, namely chitosan–thiobarbituric acid showed maximum uptake capacities of 1,357.69, 2,504.86, and 2,475.38 mg/g for respective $Hg^{\circ}$, $Hg^{2+}$, and $CH_3Hg^{+\cdot}$ and the adsorbent could be reused several times using 0.01 N thiourea, perchloric acid, and 0.2 N NaCl solutions [14]. However, this review aims to present the metal ion interaction on the raw and functionalized forms of chitosan (Fig. 1).

### 2.2 Functionalization of Chitosan with Metal Ions

Functionalization of chitosan in its amine and hydroxyl groups with various toxic-free metal ions is used for adsorption of toxic ions removal from water, which provides higher adsorption densities, hydrophilic character, and faster adsorption kinetics. Different types of metal ions were immobilized on the surface functionalities of chitosan through in situ and ex situ synthetic methods. These reactive functional groups may interact with metal ions through different mechanisms depending on the metal, the pH, and the matrix of the solution. The free-electron doublet on nitrogen may bind metal cations at pH close to neutrality (or weak acidity). The donation of lone paired electrons plays an important role in the amine–metal interaction. The interaction of metals on amine moiety present in the chitosan was studied using Raman spectroscopy and density functional theory (DFT). The most obvious change of the surface Raman spectra pattern arises from the amino group. It's interesting to note that $NH_2$ vibration modes show a significant frequency shift and an abnormal Raman enhancement in the measurements. Zhao et al. [15] have explained well about the aniline adsorption on the metal centers via Raman spectroscopy with the substantial aid of DFT calculations. In this paper, the amine–metal interaction mainly arises from the donation of amino lone pair orbital to metal unoccupied s band as described well [15]. According to Pearson's hard and soft acid-based (HSAB) concept, the hard acid metals tend to bind with hard base moieties to form a stable adduct and the same phenomenon for soft-based metals. Based on this concept, the $NH_2$ groups of chitosan considered as hard base the loading of metal ions should be hard acid behavior which leads to forming a stable interaction between them (Fig. 2).

## 3 Applications of Chitosan for Environmental Remediation

### 3.1 Fluoride Retention Using Metal–Chitosan Based Composites

Fluoride is one of the essential microelements required in trace amounts for the normal growth and development of various organs in our body more prominently bone and teeth. Fluoride is thus considered beneficial in drinking water at levels of about 0.5 mg/L but it is harmful once it exceeds 1.5 mg/L which is the World Health Organization (WHO) limit being followed in most of the nations. The Bureau of Indian standards has fixed a permissible limit of fluoride in drinking water as 1 mg/L. The excess of fluoride content in the groundwater sources is one of the major environmental health issues with the continuing growth of population and human intervention in alteration of water quality being one of the prominent causes. In India, 230 districts of 20 states are at risk of high levels of fluoride in drinking water. There are two types of fluorides: (1) ionizable/non-ionizable and (2) organic/

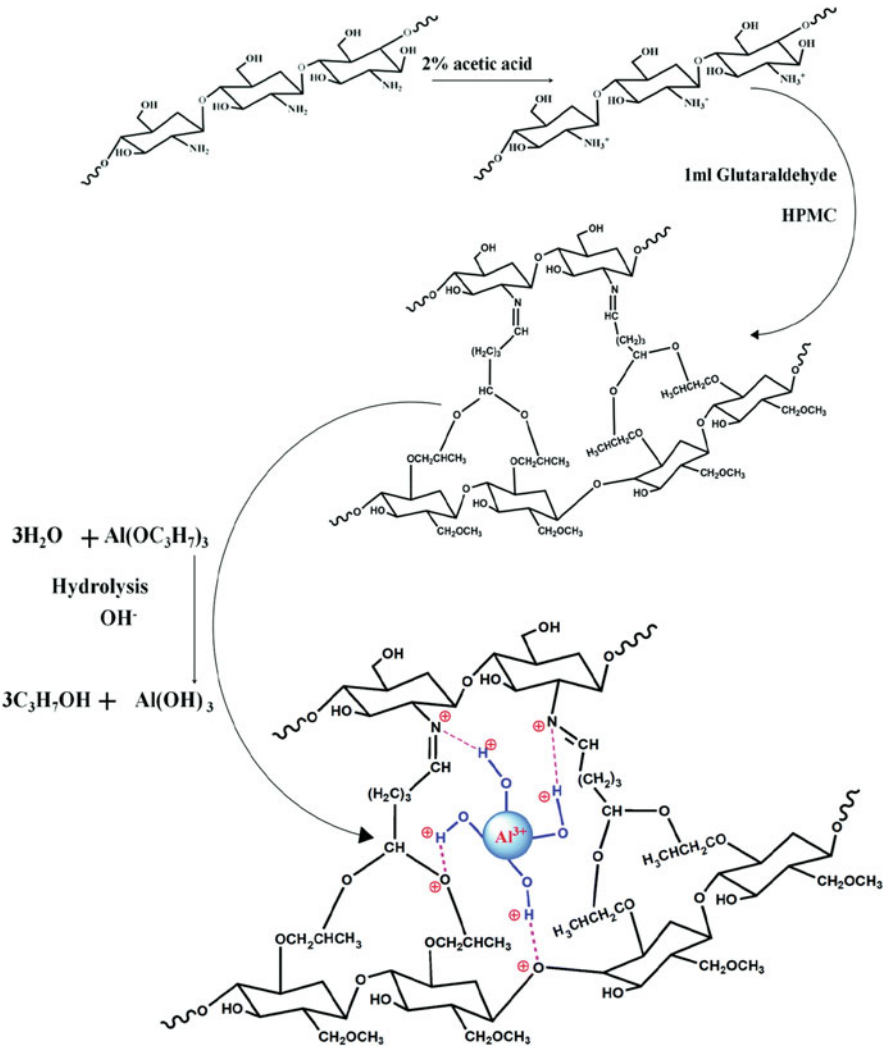


**Fig. 2** Alumina cross-linked chitosan with HPMC (hydroxypropyl methylcellulose). The figure was adapted from Ref. [16]

inorganic, in which organic fluoride does not dissolve rapidly in water until fluoride ion is released via any chemical reaction. Mostly the inorganic fluoride ions come from rock phosphates, minerals, and earth crust (950 mg/L) in its ionic form. Excessive intake of fluoride contained water may pose serious health concerns like dental, skeletal, and non-skeletal forms of fluorosis depending upon the concentration of the fluoride contents in water [17]. There are several technologies used in the defluoridation of water: reverse osmosis, nanofiltration, dialysis and electro-dialysis, and adsorption. Among them, adsorption appears to be the most appropriate solution

because it is cost-effective, simple to operate, and produces high-quality treated water [18]. Recently, chitosan-based composites using metals, metal oxides, and bimetals have been receiving large attention as alternative sorbents in water treatment processes as these kinds of materials yield high adsorption densities. To date, several successful attempts made toward the development of new materials with the maximum adsorption densities have been undertaken by employing the following strategies: (1) metal ions encapsulations, (2) magnetic nanoparticle coatings, and (3) combination of both (1) and (2) in the chitosan matrix. Viswanathan and Meenakshi have started working on chitosan and modified forms of the chitosan for fluoride removal from waters. The chemically modified forms of the chitosan, i.e., protonated and carboxylated forms beads showed excellent fluoride adsorption densities were 1.66 and 1.33 mg/L at the initial concentration of 10 mg/L [5, 19]. Then, to enhance the adsorption performance of fluoride, metal-loaded chitosan beads were prepared which showed higher adsorption densities than the protonated and carbolated forms of beads. The fluoride adsorption capacities on La- and Fe-loaded chitosan beads were 4.71 and 4.23, respectively. To continue this, La–Zr bimetallic chitosan beads were prepared by Prabhu and Meenakshi later [20], where the adsorption capacities were ~3.8 times higher than the protonated forms. Also, the material was regenerated with 0.1 M NaOH about 6 times for maximum reuse of the materials. Further, the authors have synthesized metals ($Al^{3+}$, $Ce^{3+}$, $La^{3+}$ and $Zr^{4+}$) incorporated chitosan grafted polyamidoamine dendrimers for the adsorption of fluoride from water. The results showed that Zr-loaded PAAGCB was more selective with the maximum adsorption densities of 17.47 mg/g than the other metal ions loaded PAAGCB. The thermodynamic study results indicated that the adsorption process was spontaneous and endothermic. The Zr-PAAGCB material could be effectively utilized as an adsorbent for fluoride adsorption [21]. Similar adsorption densities were obtained for magnetic materials on the chitosan matrix. The order of the magnetic materials prepared by several authors and the capacities was arranged in decreasing order as $Fe_3O_4$/chitosan/$Al(OH)_3$ beads [22] > magnetic hydrocalumite–chitosan [23] > magnetic hydrotalcite–chitosan [24] > magnetic hydroxyapatite [25]. The main advantages of these magnetic materials are easy separation of materials from solution and it suppresses separation process time and the cost of the process. Chitosan modified with highly electropositive metals and a supported material delivered high adsorption capacities. For example, Ce–chitosan (153 mg/g), *Aloe vera* supported Nano Zr chitosan [26] and Al–chitosan–hydroxypropyl methylcellulose [27]. The *Aloe vera* supported Zr nanoparticles were prepared by a simple method. The extract of *Aloe vera* was used as a reducing agent to develop Zr nanoparticles and further the nanoparticles were embedded in the chitosan matrix. Recently, a record high adsorption densities of fluoride were obtained by Affonso et al. [28] using carbon nanotube functionalized with chitosan sponge from effluent of fertilizer production industry. These adsorbents have shown a record high maximum adsorption density of 975.4 mg/g based on the kinetic and freundlich isotherm analysis results. The high adsorption caapacity was attributed to the chitosan functional groups and the high interaction area promoted by sponge form and the carbon nanotube. Additionaly, the material was reused for about

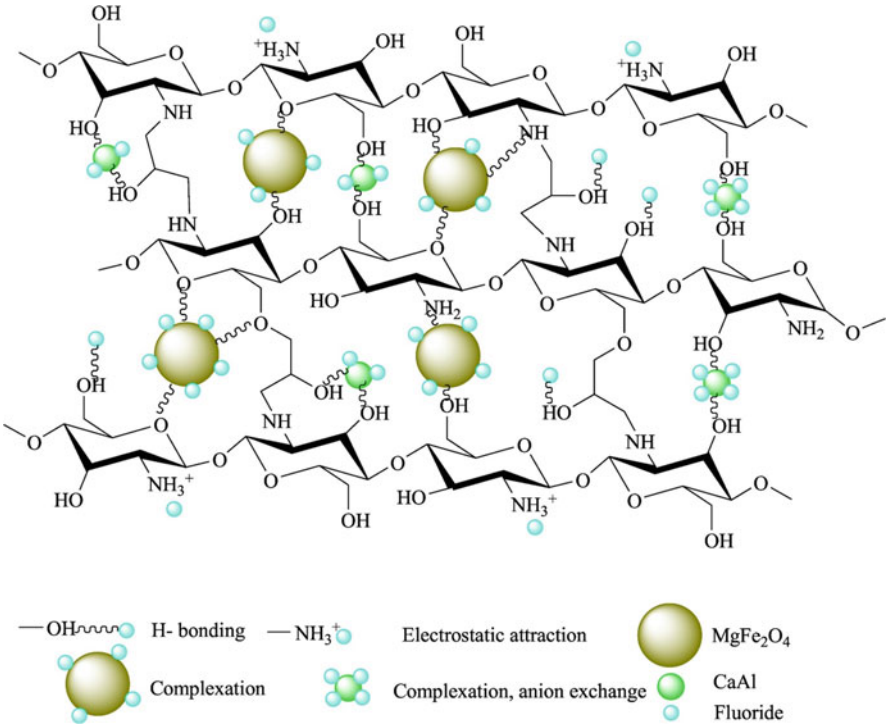


**Fig. 3** A schematic illustration of fluoride adsorption mechanism onto the magnetic MgFe2O4–chitosan–CaAl composite. The figure was adapted with permission from Ref. [27]

5 times with the aid of 0.1 M NaOH solution as an eluent [28]. Mostly the developed materials for fluoride adsorption were regenerated with NaOH with the cycles range between 5 and 10 (Fig. 3). As a result, the metal-incorporated chitosan composites proved to be more efficient adsorbents than their chemically modified counterparts. The other chitosan-based materials reported for fluoride sorption are displayed in Table 1.

## *3.2 Newly Developed Chitosan-Derivatives for Arsenic Adsorption*

Arsenic exists as oxides in soil, sediments, and water in many parts of the world and originates from both natural and anthropogenic processes. Arsenic existed in four different types of states as −3, +3, 0, and +5, in which +3 form, called arsenite ($H_3ASO_3$, As(III)) and arsenate ($HAsO_4^{2-}$, As(V)) occurs naturally in predominant forms. Arsenite is more toxic (50 times) than arsenate due to the less mobility in the

**Table 1** Functionalized forms of chitosan for fluoride removal from water

| S. No. | Adsorbent material | Fluoride adsorption capacity (mg/g) | Regeneration eluent | Regeneration cycles | Isotherm model | Kinetics | Ref. |
|---|---|---|---|---|---|---|---|
| 1 | Protonated chitosan beads | 1.66 | 0.1 M HCl | – | Langmuir–Freundlich | Pseudo-second-order | [5] |
| 2 | Carboxylated chitosan beads | 1.39 | 0.1 M HCl | – | Langmuir–Freundlich | Pseudo-second-order | [19] |
| 3 | La–chitosan beads | 4.71 | – | – | Freundlich | Pseudo-seond-order | [29] |
| 4 | Fe–chitosan beads | 4.23 | – | – | Freundlich | Pseudo-second-order | [30] |
| 5 | La–Zr mixed oxide–chitosan beads | 6.41 | 0.1 M NaOH | 06 | Langmuir | Pseudo-second-order | [20] |
| 6 | Zr–chitosan dendrimer beads | 17.47 | – | – | Freundlich | Pseudo-second-order | [21] |
| 7 | La–rare earth metal oxide/chitosan | 22.35 | 0.5 M NaOH | 07 | Freundlich | Pseudo-second-order | [31] |
| 8 | Chitosan–Fe(III) beads | 45.45 | 5% NaCl | 14 | Freundlich | Pseudo-second-order | [32] |
| 9 | $Fe_3O_4$/chitosan/$Al(OH)_3$ beads | 76.63 | – | – | Langmuir | Pseudo-second-order | [22] |
| 10 | Magnetic nanohydroxyapatite–chitosan | 4.77 | 0.1 M NaOH | 04 | Langmuir | Pseudo-second-order | [25] |
| 11 | Magnetic hydrotalcite–chitosan | 5.03 | 0.1 M NaOH | 05 | Langmuir | Pseudo-second-order | [24] |
| 12 | La–silica gel/chitosan | 4.90 | – | – | Langmuir | Pseudo-second-order | [33] |
| 13 | Magnetic hydrocalumite–chitosan | 6.80 | – | – | Langmuir | Pseudo-second-order | [23] |
| 14 | Bentonite clay/chitosan | 9.80 | 0.1 M NaOH | 05 | Freundlich | | [34] |

(continued)

**Table 1** (continued)

| S. No. | Adsorbent material | Fluoride adsorption capacity (mg/g) | Regeneration eluent | Regeneration cycles | Isotherm model | Kinetics | Ref. |
|---|---|---|---|---|---|---|---|
| | | | | | | Pseudo-second-order | |
| 15 | Chitosan–polyaniline/zirconium | 8.71 | 0.1 M NaOH | 05 | Freundlich | Pseudo-second-order | [35] |
| 16 | $Zr^{4+}$-chitosan/gelatin composite | 12.13 | 0.05 M NaOH | 05 | Langmuir | Pseudo-second-order | [36] |
| 17 | La–synthetic resin@chitosan | 17.50 | 0.01 M NaOH | 06 | Freundlich | Pseudo-second-order | [37] |
| 18 | Al–La oxyhydroxides–chitosan | 49.54 | 0.1 M NaOH | 05 | Freundlich | Pseudo-second-order | [38] |
| 19 | Fe–Al–Mn oxyhydroxide–chitosan | 55 ± 0.5 | – | – | Freundlich | Pseudo-second-order | [39] |
| 20 | Silica/chitosan | 58.80 | 1 M NaOH | 10 | Langmuir | Pseudo-second-order | [40] |
| 21 | *Aloe vera* supported Nano Zr chitosan | 96.58 | 0.1 M NaOH | 10 | Langmuir | Pseudo-second-order | [26] |
| 22 | Al–chitosan–hydroxypropyl methyl cellulose | 125.1 | Methanol | 04 | Langmuir | Pseudo-second-order | [16] |
| 23 | Ce–chitosan composite | 153.3 | 2 M NaOH | 03 | Langmuir | Pseudo-second-order | [41] |
| 24 | $MgFe_2O_4$–chitosan–CaAl composite | 263.15 | 0.1 M NaOH | 05 | Langmuir | Pseudo-second-order | [27] |
| 25 | Carbon nanotube/chitosan sponge | 975.4 | 0.1 M NaOH | 05 | Freundlich | Pseudo-first-order | [28] |

water. The chemistry of arsenic and its toxicity was well explained in the previous review article by Hao et al. [42]. The maximum permissible limit of arsenic in groundwater is 10 μg/L, described by WHO. The removal mechanisms of the toxic inorganic pollutants on chitosan adsorbents are controversial with theories including chemisorption and complexation. It is reported that the uptake of arsenic on amine moiety in chitosan through coordination with unprotonated amine groups and the protonated form of amine groups would tend to adsorb arsenic via an electrostatic interaction at different pH conditions [43]. Chitosan in its unmodified form had lower adsorption capacities than the metal incorporated chitosan moiety due to its lack of active sites for adsorption as listed out in Table 2. Kwok et al. have reported the mechanisms of arsenic removal on chitosan and nano chitosan in detail at different pH conditions and the adsorption–desorption behavior for arsenic at various eluents [43]. Further, the unmodified chitosan was used for the removal of arsenite and arsenate ions from water at pH 5 and found that the maximum adsorption densities were 1.83 and 1.94 mg/g, respectively. The chitosan was regenerated with 0.5–0.1 M $H_2SO_4$ for about 15 cycles, which is far preferable to the mere three cycles afforded by coconut husk carbon in arsenic recovery [44]. To improve its adsorption capacities, the chitosan was modified with chelating resins, and the densities were improved drastically to 62.42 mg/g with pseudo-second-order kinetic models for arsenate removal, and the materials were regenerated using 0.2 M NaOH and utilized materials for further five times with maximum adsorption densities. Metal impregnation is proposed to increase arsenic uptake capacity and favor chitosan selectivity over other metal ions and co-ions. The metals such as lanthanum, zirconium, iron, molybdenum, aluminum, and manganese are known to form complexes with arsenic ions and for their strong affinity for chitosan [45]. Salih et al. [54] have recently reported chitosan/diatomaceous composite beads as an effective adsorbent for the removal of toxic ions from water. The binary maximal adsorption densities of As(III) and As(V), as determined from the Langmuir isotherms were 87.81 and 44.07 at a pH 6, respectively. The presence of phosphate as co-existing anions has an obvious impact on the adsorption of arsenic species due to isomeric forms of phosphate and arsenic. In the desorption experiments, the chitosan/diatomaceous composite beads were examined using 0.2 M NaOH as an eluent and the adsorbents were reused for five consecutive cycles and the losses in bead mass after 5 regeneration cycles were measured as approximately 8% and 11% for As(III) and As(V) loaded beads, respectively. Likewise, a microsphere using iron-loaded chitosan was prepared by Lin et al. (2019) for the removal of toxic As(III) ions from water [46]. The As(III) ions tend to bind with the Fe-rich surface of chitosan through electrostatic interaction at acidic pH conditions and over pH 8, the result was contrary, the excess of –OH ions would compete with arsenite ions and the densities were decreased. The mechanisms of interaction was confirmed by FTIR and XPS studies, in which the FTIR studies confirmed that the presence of NH stretching vibration mode was shifted to 1,371 $cm^{-1}$ from 1,387 $cm^{-1}$ and a new peak was observed at 819 $cm^{-1}$ corresponded to Fe-O-As after adsorption. The magnetic chitosan bead and composie were made by two different groups and found that the adsorption densities were higher at compoiste form rather the beads, due to higher

**Table 2** Adsorbents used for the removal of arsenite and arsenate from waters

| S. No. | Adsorbent material | Adsorption capacity (mg/g) | | Regeneration eluent | Regeneration Cycles | Isotherm model | Kinetics | Ref. |
|---|---|---|---|---|---|---|---|---|
| | | Arsenite | Arsenate | | | | | |
| 1 | Chitosan | 1.83 | 1.94 | 0.5–0.1 M $H_2SO_4$ | 15 | – | First-order | [44] |
| 2 | Chitosan-chelating resin | – | 62.42 | 0.2 M NaOH | 05 | Langmuir | Pseudo-second-order | [49] |
| 3 | α-Fe2O3 impregnated chitosan beads | 9.355 | – | 0.5 M HCl | 10 | Langmuir | Pseudo-second-order | [50] |
| 4 | Chitosan/PVA/$Fe^0$ | 142.9 | 200.0 | 0.01 M NaOH | 05 | Langmuir | – | [51] |
| 5 | Magnetic chitosan beads | 35.7 | 35.3 | 0.1 M NaOH | 05 | Langmuir | Pseudo-second-order | [52] |
| 6 | Zr–chitosan composite | – | 190.0 | 0.5 M NaOH | 06 | Langmuir | Pseudo-second-order | [53] |
| 7 | Fe–chitosan microsphere | 95.97 | – | 1.0 M NaOH | 03 | Freundlich | Pseudo-first-order | [46] |
| 8 | Chitosan/diatomaceous | 87.81 | 44.07 | 0.2 M NaOH | 05 | Langmuir | Pseudo-second-order | [54] |
| 9 | Fe–chitosan/ZnO@ alginate microsphere | – | 63.69 | | 05 | Langmuir | Pseudo-second-order | [55] |
| 10 | $Fe_3O_4$–chitosan composite | 73.69 | 79.49 | 0.1 M NaOH | 05 | Langmuir | Pseudo-second-order | [56] |
| 11 | Magnetic chitosan bead | – | 65.5 | $Na_2EDTA$ | 05 | Langmuir | Pseudo-second-order | [57] |
| 12 | Chitosan-iron oxide films | – | 33.87 | – | – | Freundlich | Pseudo-first-order | [58] |
| 13 | Ionotropic chitosan microspheres | – | 120.77 | – | – | Langmuir | Pseudo-second-order | [59] |
| 14 | Chitosan–Fe–Al LDH@rGO | – | 167.79 | 1.0 M NaOH | 04 | Langmuir | Pseudo-second-order | [47] |

| | | | | | | | | |
|---|---|---|---|---|---|---|---|---|
| 15 | Goethite/GO/chitosan composite | 289.42 | – | 0.5 M NaOH | 05 | Freundlich and Sips | Pseudo-second-order | [48] |
| 16 | Molybdate loaded chitosan beads | – | 75.0 | 0.1 M phosphoric acid | 03 | Langmuir | Pseudo-second-order | [60] |
| 17 | Lanthanum–chitosan nanofiber | – | 83.6 | 8% in mass NaOH | 02 | Langmuir | Pseudo-seond-order | [61] |
| 18 | Chitosan–diatomite | – | 11.95 | 0.1 M NaOH | 06 | Langmuir | Pseudo-second-order | [62] |
| 19 | Fe–Mn@ chitosan/alginate | 24.06 | – | NaOH | 04 | Freundlich | Pseudo-second-order | [63] |
| 20 | Fe–chitosan | – | 14.95 | 1% NaOH | 04 | Langmuir | Pseudo-second-order | [64] |
| 21 | Fe–chitosan nanosheets | 108.6 | – | 0.5 M NaOH | 04 | Langmuir | Pseudo-second-order | [65] |
| 22 | Chitosan–$Zr_xAl_{1-x}OOH$ composite | 69.90 | – | 0.1 M NaOH | 04 | Langmuir | Pseudo-second-order | [66] |
| 23 | Chitosan–iron sand filters | 26.0 | 56.0 | – | – | Langmuir | Pseudo-first-order | |
| 24 | Chitosan–montmorillonite composites | 48.7 | – | 0.1 M $H_2PO_4$ | 03 | Freundlich | Pseudo-second-order | |
| 25 | Chitosan electrospun nanofibers | – | 11.2 | 0.003 M NaOH | 10 | Freundlich | Pseudo-second-order | |

surface area and more active sites existed in the composite form. The respective adsorption densities of arsenite and arsenate were 73.69 and 79.49 mg/g on magnetic chitosan composite which is higher adsorption densities than the magnetic chitosan beads (65.5 mg/g). Lanthanum and molybdenum ions are considered as hard acids which tend to bind with arsenate, a hard base, by well understood HSAB principle.

Bimellaic assembled chitosan materials were utilized to maximize the adsorption efficiencies of both As(III) and As(V) from waters. Recently, Priya et al. [47] have developed a material consisting of Fe–Al layered double hydroxides on chitosan with graphene oxide materials. The nanocomposite was successfully prepared by hydrothermal and ex situ polymerization process with an enhanced surface area which provides more number of active sites. The LDH moieties were attached with GO groups through electrostatic interaction and the negatively charged arsenic species interacted with this nanocomposite through coordination, ligand exchange, and electrostatic interaction mechanisms. The adsorption capacities of the materials were found to be 167.80 mg/g, which is higher than the pristine forms of the materials [47]. Another group from China has recently developed goethite/graphene oxide/chitosan nanocomposite materials for the removal of As(III) from water. They found that the multifunctional groups such as NHCO, C-O, O-H, and Fe-O were responsible for adsorption of arsenite ions from water. The maximum adsorption density of 289.42 mg/g was calculated using the Langmuir isotherm model and the material was used five consecutive times with the minimal loss of its efficiencies [48].

Chitosan-supported mixed metal oxyhydroxides ($Zr_xAl_{1-x}OOH$) were prepared by Prabhu and Sasaki for the simultaneous removal of toxic fluoride and arsenite ions from single and binary solutions. A higher amount of arsenite was adsorbed in binary solutions than the single solutions, through electrostatic interaction and ligand exchange mechanisms at different pH conditions. Further, the material was supplied to remove the three-component system of natural co-existing anions and found no significant decrement in the adsorption densities. The material could be reused about four times using 0.1 M NaOH as an eluent. Again bimetallic rich chitosan–alginate biopolymeric nanocomposite was developed by Zeng et al. (2020) that materials showed a surface area of 128.16 $m^2/g$ and showed maximum efficiencies of 24.06 mg/g [63]. The mechanism of attraction of arsenic by complexation and the desorption by NaOH could be used for four adsorption and desorption cycles (Fig. 4). The other materials used for the removal of toxic arsenite and arsenate using chitosan-based materials are listed in Table 2.

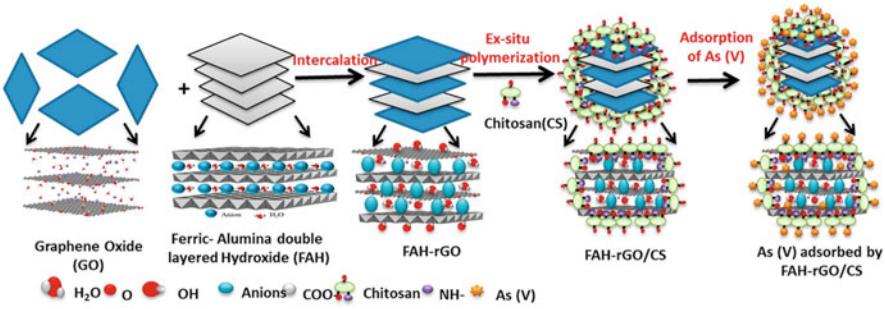


**Fig. 4** A schematic view of mechanism of intercalation and ex situ polymerization of chitosan and its adsorption of arsenate from water. The figure was adapted with permission from Ref. [47]

## *3.3 Metal and Metal-Free Chitosan Materials for Phosphate and Nitrate Adsorption*

The nutrients pollution in a water body such as nitrogen and phosphorus are serious environmental issues worldwide. The dissolved nutrients species ammonium, nitrate, and phosphate are particularly important pollutants, resulting in aquatic eutrophication, which is an abundance of aquatic plants, growth of algae, and depletion of dissolved oxygen [67]. The nitrate ion in drinking water is 40 mg/L set by WHO, when it exceeds causes public health hazards including infant methemoglobinemia called Blue baby syndrome and the other forms of carcinogenic nitrosamines and nitrosamides. Agricultural fertilizers, aquaculture, agri-food industries, municipal wastewaters, and detergent manufacturing industries are the main sources of nitrate and phosphate release in the waterbody. Also, thermal power plants discharge their wastes into water that contains large amounts of nitrate ions [68]. A lot of materials were tried to remove the maximum amount of nitrate and phosphate ions through adsorption method. A few review articles explained well the materials used for the removal of those ions from water. This review is currently updating the chitosan-based materials used for the removal of phosphate and nitrate ions from water. Kumar et al. [69] investigated the $NO_3^-$ and $PO_4^{3-}$ adsorption properties of chitosan encapsulated lanthanum oxide admixed *Aegle marmelos* ($La_2O_3$AM@CS) composite beads. The hydrothermal supported $La_2O_3$AM@CS composite beads possess the $NO_3^-$ and $PO_4^{3-}$ adsorption capacity of 27.84 and 34.91 mg/g, respectively [69]. The pH influences the $NO_3^-$ and $PO_4^{3-}$ adsorption capacity of $La_2O_3$AM@CS composite beads, and $SO_4^{2-}$ ion mainly competes with $NO_3^-$ and $PO_4^{3-}$ adsorption due to charge and size effects. They also reported that the chitosan-supported metal/bentonite composite beads viz. Zr@CSBent, La@CSBent, and Ce@CSBent for $NO_3^-$ adsorption from water. Among the studied materials, Zr@CSBent composite beads showed a higher adsorption capacity of 23.89 mg/g [70]. Banu et al. reported the $Zr^{4+}$ ions implanted chitosan–soybean husk activated bio-char composite beads (Zr-CS-SAC) for $NO_3^-$ and $PO_4^{3-}$ adsorption and possesses the maximum adsorption capacity of 90.09 and 131.29 mg/g at 30°C

[71]. Jiang et al. [72] synthesized the $Fe_3O_4/ZrO_2$/chitosan composite using a low-cost method at the mild condition. The developed $Fe_3O_4/ZrO_2$/chitosan composite has an adsorption capacity of 89.3 mg/g and 26.5 mg P/g for $NO_3^-$ and $PO_4^{3-}$, respectively [72]. Karthikeyan et al. developed the lanthanum-loaded chitosan membrane (La@CS) by casting technique, and the La@CS membrane showed the $PO_4^{3-}$ and $NO_3^-$ adsorption capacity of 76.6 and 62.6 mg/g, respectively [73]. The same authors also developed $Fe^{3+}$ cross-linked chitosan/alginate (Fe-CS-Alg) hybrid beads for $PO_4^{3-}$ and $NO_3^-$ from an aqueous solution and having the maximum adsorption capacity of 84.74 and 69.10 mg/g, respectively [74]. Further, they moved to prepare the cerium loaded chitosan-β-cyclodextrin (Ce-CS-β-CD) microspheres and applied for the removal of $PO_4^{3-}$ and $NO_3^-$, which exhibited the excellent adsorption capacity of 88.54 and 72.12 mg/g for $PO_4^{3-}$ and $NO_3^-$, respectively [75]. They also prepared zirconium fixed chitosan–starch membrane (Zr-CS-ST) for $PO_4^{3-}$ and $NO_3^-$ removal, which possesses the adsorption capacities of 86.28 and 70.88 mg/g, respectively [76]. An environmentally friendly $Al^{3+}$ incorporated chitosan and gelatin (Al@CS-Ge) microspheres were fabricated by Karthikeyan et al. [77] and utilized as an effective adsorbent for the removal of $PO_4^{3-}$ and $NO_3^-$. The main interaction between the two biopolymeric materials entrapped with metal ions would tend to adsorb more nitrate and phosphate ions due to the availability of the active sites for adsorption. The electrostatic interaction, complexation, and ion-exchange mechanisms were the mainly governed factors for adsorption of nitrate and phosphate ions from waters [77]. Kim et al. [78] have applied iron oxide nanoparticle–chitosan (ION-chitosan) composites for $PO_4^{3-}$ removal from the natural water. The ION-chitosan composite is not pH sensitive between the pH values of 5.0 to 9.0 and has the $PO_4^{3-}$ removal capacity of 0.059 mg P/g [78]. Kumar and Viswanathan prepared multivalent metal ions like $Zr^{4+}$, $Fe^{3+}$, and $Ca^{2+}$ cross-linked chitosan bentonite composites Zr@CSBent, Fe@CSBent, and Ca@CSBent, respectively. The developed composites possess the efficient $PO_4^{3-}$ adsorption capacities of 40.86, 22.15, and 13.44 mg/g than the specific CSBent composite [79]. The $Zr^{4+}$-imprinted chitosan (CCP-Zr) was prepared by forming-membrane and cross-linking method by Liu et al. [80]. The CCP-Zr have the maximum monolayer adsorption capacity of 71.68 mg/g at pH 3 and 30°C [80]. The chitosan beads modified with zirconium (ZCB) were developed by Liu and Zhang for $PO_4^{3-}$ removal from an aqueous medium, which possesses the maximum monolayer adsorption capacity of 60.6 mg/g [81]. Mahaninia and Wilson cross-linked the chitosan beads with glutaraldehyde and epichlorohydrin and used for the removal of phosphate dianion ($HPO_4^{2-}$) from an aqueous solution at pH 8.5 and 22°C and possesses adsorption capacity of 22.4–52.1 mg/g [82]. Nthumbi et al. [83] prepared chitosan/polyacrylamide nanofibers and used them for the removal of $PO_4^{3-}$. The nanofibers had an adsorption capacity of 392 mg/g and removal efficiencies of 97.4% in synthetic and field water samples [83]. Sowmya and Meenakshi have developed various types of chitosan-based adsorbent materials

including quaternized chitosan beads (QCB) [84], hydrotalcite/chitosan (HT/CS) composite, quaternized chitosan–melamine–glutaraldehyde resin (QCMGR) [85], protonated a carboxylated cross-linked chitosan bead (PCB), (CCB) [86], La(III)-loaded silica-chitosan composite (LSCC) [87], Zr(IV) cross-linked chitosan beads (ZrCB) [88], zinc-loaded cross-linked chitosan beads (ZnCB) and zinc-loaded carboxylated cross-linked chitosan beads (ZnCCB) for the removal of both $PO_4^{3-}$ and $NO_3^-$ from water [89]. The reported the adsorbent materials possess very good adsorption capacity for the removal of $PO_4^{3-}$ and $NO_3^-$ from synthetic and real-water samples. The LSCC material exhibited the highest affinity for phosphate removal and nitrate removal from water out of all the developed materials. Based on this scenerio, Banu et al. (2018) [90] synthesized the $La^{3+}$-incorporated chitosan–montmorillonite composite (La-CS-MMT) for the effective removal of $PO_4^{3-}$ from aqueous solution, which successfully removed 92% of the $PO_4^{3-}$ within 30 min. By electrostatic attraction, the phosphate ions were adsorbed on La-CS-MMT to form an outer-sphere complex, as confirmed by the D-R isotherm, and the adsorbed material was then desorbed with 0.1 M NaOH. In regard to MMT and CS, hydrogen bonding is a common mechanism for their interaction with phosphate and nitrate. Zavareh et al. [91] reported the magnetic Cu–chitosan/$Fe_3O_4$ nanocomposite for selective and effective removal of $PO_4^{3-}$. The synthesized magnetic adsorbent has the maximum adsorption capacity of 88 mg $P_2O_5$/g, which is higher than the neat chitosan and chitosan/$Fe_3O_4$ according to the Langmuir isotherm [91]. Kumar and Viswanathan have prepared the tetra amine copper(II) salt grafted chitosan (TAC@CS) composite beads for $PO_4^{3-}$ adsorption, and the TAC@CS composite beads posses the enhanced adsorption capacity of 41.42 ± 0.071 mg/g compared to other prepared adsorbent materials [92]. Kumar and Viswanathan have developed magnetic adsorbents like amine-grafted magnetic gelatin (AGMGel) composite, magnetic-chitosan-assisted hydrotalcite (MCSHT), and magnetic-alginate-assisted hydrotalcite (MAlgHT) composite beads for the adsorption of $NO_3^-$ and $PO_4^{3-}$ from water. The researchers also synthesized zirconium oxyhydroxide (Zr@CSKN) composite by hydrothermal method for enhanced nitrate and phosphate adsorption [93–95].

Zhao and Feng reported the modified chitosan beads for $PO_4^{3-}$ and $NO_3^-$ adsorption with different pH, the initial concentration, contact time, and adsorbent dosage. The results displayed that modified chitosan beads are an excellent adsorbent for the removal of $NO_3^-$ and $PO_4^{3-}$ with an adsorption capacity of 32.15 and 33.90 mg/g, respectively [96]. Golie and Upadhyayula have synthesized chitosan/bentonite, chitosan/titanium oxide, and chitosan/alumina (ChBT, ChTi, and ChAl, respectively) for $NO_3^-$ adsorption from aqueous solution by batch biosorption experiments, and the composites possess the adsorption capacity of 35.68 and 43.62 and 45.38 mg/g, respectively [97]. Banu and Meenakshi reported the one-pot synthesis of chitosan grafted quaternized resin for the removal of $NO_3^-$ and $PO_4^{3-}$ from water. The removal efficiency of $NO_3^-$ and $PO_4^{3-}$ on chitosan quaternized resin was 78% and 90%, respectively, with 0.1 g of adsorbent and the initial concentration as 100 mg/L [98]. A granular chitosan–$Fe^{3+}$ complex with high chemical stability and good environmental adaptation was developed by Hu et al.

and used for the adsorption of $NO_3^-$ and possesses the adsorption capacity of 8.35 mg $NO_3$–N/g based on Langmuir–Freundlich model [99]. Zhang et al. (2018) and Zhao et al. (2020) have developed the composites like Fe(III)-doped chitosan (CTS-Fe) [100] and cross-linked Fe(III)-chitosan (CTS-Fe-CL) [101] for the removal of phosphorus. The maximum phosphate adsorption capacity for CTS-Fe and CTS-Fe-CL was 15.7 and 10.2 mg P/g at 30°C, respectively. Lanthanum-chitosan hydrogel coated with polydopamine (La-CS@PDA) was synthesized with abundant amino groups, and the composite followed the Langmuir isotherm model with an adsorption capacity of 195.3 mg/g. Chitosan/Zeolite Y/Nano $ZrO_2$ nanocomposite adsorbent was synthesized by Teimouri et al. [102] and applied for the removal of $NO_3^-$ from the aqueous solution. The $NO_3^-$ adsorption process was described by Langmuir isotherm model with the adsorption capacity of 23.58 mg/g [102].

The nanochitosan-graphene oxide composite (NCS@GO) was prepared by Salehi and Hosseinifard, which is examined for adsorption of $PO_4^{3-}$ and $NO_3^-$ from aqueous solutions. The zirconium loading was optimized in NCT@GO composite to make it selective for the adsorbate anions, and NCS@GO/H-Zr established a very good $PO_4^{3-}$ and $NO_3^-$ uptake of 172.41 mg P/g and 138.88 mg N/g, respectively. The removal capacity of P and N anions was also assessed in bi-component systems and the Freundlich isotherm fitted well, suggesting the multilayer formation. Real samples analysis indicated that the prepared material works well for the removal of P and N anions from contaminated waters [103]. Yazdani et al. [104] reported the zinc (II)$^-$chitosan complexes as a bio-sorbent for $PO_4^{3-}$ removal from aqueous solutions. The zinc(II) ions into chitosan expand its performance towards $PO_4^{3-}$ removal from 1.45 to 6.55 mg/g. Using functionalized nanochitosan/clinoptilolite (Nano-CS/Clino) composites, nitrate ions were removed from water. The Nano-CS/Clino@PEHA composite was found to have a higher nitrate adsorption capacity of 277.77 mg/g than Nano-CS/Clino@H (227.27 mg/g) and Nano-CS/Clino (185.18) [104, 105]. More recently, Fu et al. [106] developed the polyethylenimine-grafted chitosan core-shell ($Fe_3O_4$/CS/PEI) magnetic nanoparticles and utilized them for adsorbing $PO_4^{3-}$ in water. The adsorption isotherms of $PO_4^{3-}$ on $Fe_3O_4$/CS/PEI particles were well fit by the Langmuir equation, and its maximum adsorption was 48.2 mg/g at an equilibrium pH of 3.0 and 25°C [106]. Non-cross-linked lanthanum-chitosan (La-CTS-0X) and cross-linked lanthanum-chitosan (La-CTS-1X/2X) composites were prepared as new complex biosorbents for effective $PO_4^{3-}$ removal from wastewater by Liu et al. [107]. The maximum $PO_4^{3-}$ adsorption capacity for La-CTS-0X/1X/2X was 47.28, 57.84, and 31.01 mg/g at pH 6, respectively [107].

The materials used for the removal of phosphate and nitrate were mostly regenerated with NaCl and NaOH at different concentrations depending upon the metal concentrations of composites/hybrids and the maximum re-useable cycles are between 5 and 10. The metal-loaded chitosan-based composites showed extraordinary performance than the pristine forms due to the hydroxide ions and the metal affinity towards the nitrate and phosphate ions from water. The quarternized forms of

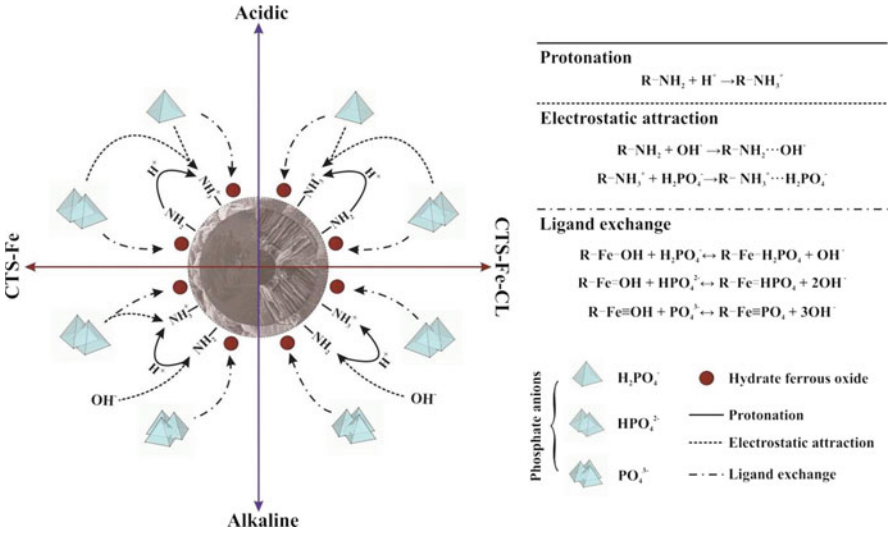


**Fig. 5** Mechanism of phosphate adsorption using Fe(III)-doped chitosan and cross-linked Fe(III)-doped chitosan. The figure was adapted with permission from Ref. [100]

chitosan materials attract phosphate and nitrate ions through a ligand-exchange mechanism which can be confirmed by an ion-chromatogram, where the $Cl^-$ ions concentrations can measure periodically and the phosphate and nitrate ions concentration can be measured simultaneously (Fig. 5 and Table 3).

## 4 Summary and Outlooks

Recently, studies have proposed the synthesis of novel, new, and eco-friendly nanomaterials that use adsorbent technologies to remove toxic ions from waters and wastewaters. Overall, the reported materials with the background of chitosan showed ultra-high adsorption densities toward the removal of fluoride, arsenic, phosphate, and nitrate ions from water under batch experiments. Mostly, the materials used for this review were prepared by conventional method and a few of them were synthesized by in situ and ex situ synthetic methods which significantly improved the stability of the materials. Besides, the surface area of the materials was also enhanced due to the synergistic interaction of the active material with the chitosan background. At different pH levels, the mechanisms of interactions with toxic ions include electrostatic interactions, inner-and outer-sphere complexation, and ligand exchange. Despite the wide applications were adopted for new generation material for the removal of fluoride, arsenic, phosphate, and nitrate from water, some drawbacks still exist.

**Table 3** Removal of phosphate and nitrate ions from water using chitosan-based sorbents

| S. No. | Adsorbent material | Adsorption capacity | | Regeneration eluent | Regeneration cycles | Isotherm | Kinetics | Ref. |
|---|---|---|---|---|---|---|---|---|
| | | Phosphate (mg/g) | Nitrate (mg/g) | | | | | |
| 1 | Chitosan Encapsulated lanthanum oxide | 34.91 | 27.84 | NaOH | 6 | Freundlich | – | [69] |
| 2 | $Zr^{4+}$, $La^{3+}$, and $Ce^{3+}$ cross-linked chitosan assisted bentonite composite | – | 23.89, 19.54 and 16.63 | 0.01 M NaOH | 6 | Freundlich | Pseudo-first-order | [70] |
| 3 | $Zr^{4+}$ ions embedded chitosan–soybean husk activated bio-char composite beads | 131.29 | 90.09 | 0.1 M NaCl | 5 | Freundlich | Pseudo-first-order | [71] |
| 4 | $Fe_3O_4/ZrO_2$/chitosan composite | 26.5 | 89.3 | – | – | Langmuir | Pseudo-first-order | [72] |
| 5 | Lanthanum incorporated chitosan membrane | 76.6 | 62.6 | 0.1 M NaOH | 5 | Freundlich | Pseudo-first-order | [73] |
| 6 | $Fe^{3+}$ loaded chitosan and alginate biopolymeric hybrid beads | 84.74 | 69.10 | 0.1 M NaOH | 5 | Freundlich | Pseudo-first-order | [74] |
| 7 | Cerium incorporated chitosan-β-cyclodextrin | 88.54 | 72.12 | 0.1 M NaOH | 5 | Freundlich | Pseudo-first-order | [75] |
| 8 | Zirconium entrenched chitosan-starch membrane | 86.28 | 70.88 | 0.1 M NaOH | 5 | Freundlich | Pseudo-first-order | [76] |
| 9 | $Al^{3+}$ incorporated chitosan and gelatin microspheres | 90.14 | 74.15 | 0.1 M NaOH | 5 | Freundlich | Pseudo-first-order | [77] |
| 10 | Iron oxide nanoparticle-loaded chitosan composites | 0.059 | – | 0.001 M NaOH | 6 | Freundlich | Pseudo-second-order | [78] |
| 11 | $Zr^{4+}$, $Fe^{3+}$, and $Ca^{2+}$ chitosan-supported bentonite composite | 40.86, 22.15, and 13.44 | – | – | – | Freundlich | Pseudo-first-order | [79] |

| | | | | | | | | |
|---|---|---|---|---|---|---|---|---|
| 12 | Zirconium (IV) loaded cross-linked chitosan | 71.68 | – | – | – | Langmuir | Pseudo-first-order | [80] |
| 13 | Zirconium(IV) modifying chitosan biocomposite | 61.7 | – | 0.5 M NaOH | 5 | Langmuir | Pseudo-first-order | [81] |
| 14 | Cross-linked Chitosan beads | 52.1 | – | 0.05 M NaCl | 4 | Sips | – | [82] |
| 15 | Chitosan/polyacrylamide nanofibers | 392.0 | – | 2.0 M HCl | – | Freundlich | Pseudo-second-order | [83] |
| 16 | Quaternized chitosan beads | 59.0 | 67.5 | 0.025 M NaCl | 10 | Freundlich | Pseudo-second-order | [84] |
| 17 | Hydrotalcite/chitosan composite | 57.87 | – | – | – | Freundlich | Pseudo-second-order | |
| 18 | Chitosan–melamine–glutaraldehyde resin | 112.5 | 97.5 | 0.025 M NaCl | 10 | Freundlich | Pseudo-second-order | [85] |
| 19 | Protonated cross-linked chitosan beads (PCB) and carboxylated cross-linked chitosan beads | 58.5 & 48.8 | 113.1 & 90.6 | 0.1 M NaOH | 5 | Freundlich | Pseudo-second-order | [86] |
| 20 | Lanthanum-loaded chitosan-silica and lanthanum-loaded chitosan materials | 155.4 84.2 | – | 0.25 M NaOH | 5 | Freundlich | Pseudo-second-order | [87] |
| 21 | Zr(IV) was loaded in the cross-linked chitosan beads | 69.54 | 250.63 | 0.025 M NaCl | 10 | Freundlich | Pseudo-second-order | [88] |
| 22 | Zn(II) loaded chitosan beads and Zn(II) loaded carboxylated chitosan beads | 59.00 and 67.50 | 27.56 and 31.45 | 0.025 M NaCl | 5 | Freundlich | Pseudo-second-order | [89] |

(continued)

**Table 3** (continued)

| S. No. | Adsorbent material | Adsorption capacity | | Regeneration eluent | Regeneration cycles | Isotherm | Kinetics | Ref. |
|---|---|---|---|---|---|---|---|---|
| | | Phosphate (mg/g) | Nitrate (mg/g) | | | | | |
| 23 | Lanthanum (III) encapsulated chitosan-montmorillonite composite | 128.5 | – | 0.1 M NaOH | 5 | Freundlich | Pseudo-second-order | [90] |
| 24 | Cu–chitosan/$Fe_3O_4$ Nanocomposite | 88.0 | – | $CuSO_4$ | 5 | Langmuir and Freundlich | Pseudo-second-order | [91] |
| 25 | Tetra-amine copper(II) chitosan beads | 41.42 | – | 0.25 M NaOH | 4 | Freundlich | Pseudo-second-order | [92] |
| 26 | Modified chitosan microspheres | 33.90 | 32.15 | 0.1 M NaOH | 4 | Langmuir | Pseudo-second-order | [96] |
| 27 | Chitosan/bentonite, chitosan/titanium oxide, and chitosan/ alumina composite | – | 45.38 | NaCl | 7 | Freundlich | Pseudo-second-order | [97] |
| 28 | Chitosan quaternized resin | 30.4 | 23.7 | 0.1 M NaCl | 7 | Freundlich | Pseudo-second-order | [98] |
| 29 | Amine-grafted chitosan hybrid beads | 42.95 | 38.40 | 0.1 M NaOH | 8 | Freundlich | Pseudo-second-order | [93] |
| 30 | Zirconium oxyhydroxide capped chitosan/kaolin framework | 38.34 | 31.83 | 0.025 M NaOH | 6 | Freundlich | Pseudo-second-order | [94] |
| 31 | Magnetic-chitosan-assisted hydrotalcite beads | 35.98 | – | 0.1 M NaOH | 6 | Freundlich | Pseudo-second-order | [95] |

| | | | | | | | | |
|---|---|---|---|---|---|---|---|---|
| 32 | Chitosan–$Fe^{3+}$ complex | – | 8.35 | 0.1 M NaCl | – | Langmuir–Freundlich | Pseudo-second-order | [99] |
| 33 | Fe(III)-doped chitosan and cross-linked Fe(III)-chitosan composites | – | 15.7 and 10.2 | 0.5 M NaOH | 5 | Freundlich | Pseudo-second-order | [100] |
| 34 | Chitosan/zeolite Y/Nano zirconium oxide nanocomposites | – | 23.58 | – | – | Langmuir | Pseudo-second-order | [102] |
| 35 | Zirconium functionalized nanochitosan-graphene oxide composite | 172.41 | 138.88 | 0.5 M $Na_2CO_3$ | 10 | Freundlich | Pseudo-second-order | [103] |
| 36 | Zinc(II)–chitosan complexes | 7.37 | – | – | – | Sips | Pseudo-second-order | [104] |
| 37 | Nanochitosan/clinoptilolite pentaethylene–hexamine composite | – | 277.77 | 1 M NaOH | 3 | Freundlich | Pseudo-second-order | [105] |
| 38 | Polyethylenimine-grafted $Fe_3O_4$@ chitosan core-shell magnetic nanoparticles | 50.8 | – | 0.05 M NaOH | 5 | Langmuir | Elovich model | [106] |
| 39 | Polydopamine on lanthanum–chitosan hydrogel | 195.3 | – | 0.3 NaCl and 0.1 M NaOH mixture | 5 | Freundlich | Pseudo-second-order | [101] |
| 40 | Cross-linked lanthanum–chitosan | 57.84 | – | 0.1 M NaOH | 3 | Langmuir | Pseudo-second-order | [107] |

1. The chitosan-based materials can be easily dissolved in 1–2% acetic acid and they can be modified in various forms by adding the metal ions in it. But the adsorption takes place at acidic conditions and most of the metal ions may undergo dissolution which leads to taking the secondary treatment to recover the metal nanoparticles from water. Also, the excess loading of metal ions might block the active sites and the metal hydroxide is the only one responsible for the removal of toxic ions from water. The water quality parameters before and after the treatment were analyzed using standard methods for the determination of residual toxicity.
2. The regeneration of the chitosan-based materials is mandatory to reduce the cost factor of the process and the feasibility of the studies. Most of the studies were focused on batch adsorption and only a few were reported with column experiments. Regeneration studies of the materials were rarely reported in this study. In order to develop the model for domestic and community models, the column study can be applied to promote the next step of development. Only a few of the reported studies were focused on the recovery of adsorbed material and desorbed metals. Newly developed desorption techniques for metallic ions using recyclable chemicals reduce the consumption of concentrated acids and alkalis.
3. Real-water analysis is the fundamental factor in deciding the applicability of the adsorbent. Naturally, the groundwater contains several anions, cations that interfere with the adsorption of toxic ions from water. It is important to choose adsorbents that are able to withstand even higher concentrations of interference without affecting their adsorption capacities. After the ions were adsorbed, the adsorbents were disposed in landfills or ponds, easily contaminating water, soil, and the air is referred to as secondary pollution. The arsenic and fluoride-sorbed materials were carefully stabilized before disposed of. There are few reports about the stabilization of $Cs^{+}$, $Sr^{2+}$ using fly-ash-based zeolite materials, which helps to avoid releasing them into the environment again.
4. Adsorbents cost factors are the important parameter for practical feasibility. This will be done by comparing the cost of the method developed in the laboratory and that of other commercially available models.

**Acknowledgment** SMP would like to thank the National Research Foundation of Korea (NRF) (2020H1D3A1A04106215) for the Korea Post-doctoral fellowship program.

## References

1. Suresh PV (2012) Biodegradation of shrimp processing bio-waste and concomitant production of chitinase enzyme and N-acetyl-D-glucosamine by marine bacteria: production and process optimization. World J Microbiol Biotechnol 28:2945–2962
2. Suryawanshi N, Jujjavarapu SE, Ayothiraman S (2019) Marine shell industrial wastes–an abundant source of chitin and its derivatives: constituents, pretreatment, fermentation, and pleiotropic applications – a revisit. Int J Environ Sci Technol 16:3877–3898

3. Zhao D, Huang W-C, Guo N, Zhang S et al (2019) Two-step separation of chitin from shrimp shells using citric acid and deep eutectic solvents with the assistance of microwave. Polymers (Basel) 11:409
4. Guibal E (2004) Interactions of metal ions with chitosan-based sorbents: a review. Sep Purif Technol 38:43–74
5. Viswanathan N, Sundaram CS, Meenakshi S (2009) Removal of fluoride from aqueous solution using protonated chitosan beads. J Hazard Mater 161:423–430
6. Kousalya GN, Rajiv Gandhi M, Meenakshi S (2010) Sorption of chromium(VI) using modified forms of chitosan beads. Int J Biol Macromol 47:308–315
7. Rajiv Gandhi M, Kousalya GN, Viswanathan N, Meenakshi S (2011) Sorption behaviour of copper on chemically modified chitosan beads from aqueous solution. Carbohydr Polym 83:1082–1087
8. Pokhrel S, Yadav PN (2019) Functionalization of chitosan polymer and their applications. J Macromol Sci A 56:450–475
9. Macquarrie DJ, Hardy JJE (2005) Applications of functionalized chitosan in catalysis. Ind Eng Chem Res 44:8499–8520
10. Mincke S, Asere TG, Verheye I, Folens K et al (2019) Functionalized chitosan adsorbents allow recovery of palladium and platinum from acidic aqueous solutions. Green Chem 21:2295–2306
11. Carvalho IC, Medeiros Borsagli FGL, Mansur AAP, Caldeira CL et al (2019) 3D sponges of chemically functionalized chitosan for potential environmental pollution remediation: biosorbents for anionic dye adsorption and 'antibiotic-free' antibacterial activity. Environ Technol:1–21
12. Zarghami Z, Akbari A, Latifi AM, Amani MA (2016) Design of a new integrated chitosan-PAMAM dendrimer biosorbent for heavy metals removing and study of its adsorption kinetics and thermodynamics. Bioresour Technol 205:230–238
13. Ji J, Wang L, Yu H, Chen Y et al (2014) Chemical modifications ofcChitosan and its applications. *Polym.-Plast. Technol.* Engineering 53:1494–1505
14. Bhatt R, Kushwaha S, Bojja S, Padmaja P (2018) Chitosan–thiobarbituric acid: a superadsorbent for mercury. ACS Omega 3:13183–13194
15. Zhao L-B, Huang R, Bai M-X, Wu D-Y, Tian Z-Q (2011) Effect of aromatic amine−metal interaction on surface vibrational raman spectroscopy of adsorbed molecules investigated by density functional theory. J Phys Chem C 115:4174–4183
16. Barik B, Nayak PS, Achary LSK, Kumar A, Dash P (2020) Synthesis of alumina-based cross-linked chitosan–HPMC biocomposite film: an efficient and user-friendly adsorbent for multipurpose water purification. New J Chem 44:322–337
17. Mohapatra M, Anand S, Mishra BK, Giles DE, Singh P (2009) Review of fluoride removal from drinking water. J Environ Manage 91:67–77
18. Wambu EW, Ambusso WO, Onindo C, Muthakia GK (2015) Review of fluoride removal from water by adsorption using soil adsorbents – an evaluation of the status. J Water Reuse Desalin 6:1–29
19. Viswanathan N, Sundaram CS, Meenakshi S (2009) Sorption behaviour of fluoride on carboxylated cross-linked chitosan beads. Colloids Surf B Biointerfaces 68:48–54
20. Muthu Prabhu S, Meenakshi S (2014) Enriched fluoride sorption using chitosan supported mixed metal oxides beads: synthesis, characterization and mechanism. J Water Process Eng 2:96–104
21. Muthu Prabhu S, Meenakshi S (2015) A dendrimer-like hyper branched chitosan beads toward fluoride adsorption from water. Int J Biol Macromol 78:280–286
22. Hu H, Yang L, Lin Z, Xiang X et al (2018) Preparation and characterization of novel magnetic $Fe_3O_4$/chitosan/$Al(OH)_3$ beads and its adsorption for fluoride. Int J Biol Macromol 114:256–262

23. Pandi K, Viswanathan N, Meenakshi S (2019) Hydrothermal synthesis of magnetic iron oxide encrusted hydrocalumite-chitosan composite for defluoridation studies. Int J Biol Macromol 132:600–605
24. Pandi K, Periyasamy S, Viswanathan N (2017) Remediation of fluoride from drinking water using magnetic iron oxide coated hydrotalcite/chitosan composite. Int J Biol Macromol 104:1569–1577
25. Pandi K, Viswanathan N (2015) Synthesis and applications of eco-magnetic nano-hydroxyapatite chitosan composite for enhanced fluoride sorption. Carbohydr Polym 134:732–739
26. Prasad KS, Amin Y, Selvaraj K (2014) Defluoridation using biomimetically synthesized nano zirconium chitosan composite: kinetic and equilibrium studies. J Hazard Mater 276:232–240
27. Ghanbarian M, Ghanbarian M, Mahvi AH, Tabatabaie T (2020) Enhanced fluoride removal over $MgFe_2O_4$–chitosan–CaAl nanohybrid: response surface optimization, kinetic and isotherm study. Int J Biol Macromol 148:574–590
28. Affonso LN, Marques JL, Lima VVC, Gonçalves JO et al (2020) Removal of fluoride from fertilizer industry effluent using carbon nanotubes stabilized in chitosan sponge. J Hazard Mater 388:122042
29. Viswanathan N, Meenakshi S (2008) Enhanced fluoride sorption using La(III) incorporated carboxylated chitosan beads. J Colloid Interface Sci 322:375–383
30. Viswanathan N, Meenakshi S (2008) Selective sorption of fluoride using Fe(III) loaded carboxylated chitosan beads. J Fluor Chem 129:503–509
31. Liang P, An R, Li R, Wang D (2018) Comparison of $La^{3+}$ and mixed rare earths-loaded magnetic chitosan beads for fluoride adsorption. Int J Biol Macromol 111:255–263
32. Tandekar S, Saravanan D, Korde S, Jugade R (2020) Gamma degraded chitosan-Fe(III) beads for defluoridation of water. Mater Today: Proc 29:726–732
33. Viswanathan N, Pandi K, Meenakshi S (2014) Synthesis of metal ion entrapped silica gel/chitosan biocomposite for defluoridation studies. Int J Biol Macromol 70:347–353
34. Nagaraj A, Pillay K, Kishor Kumar S, Rajan M (2020) Dicarboxylic acid cross-linked metal ion decorated bentonite clay and chitosan for fluoride removal studies. RSC Adv 10:16791–16803
35. Muthu Prabhu S, Meenakshi S (2016) Defluoridation of water using dicarboxylic acids mediated chitosan-polyaniline/zirconium biopolymeric complex. Int J Biol Macromol 85:16–22
36. Preethi J, Karthikeyan P, Vigneshwaran S, Meenakshi S (2021) Facile synthesis of $Zr^{4+}$ incorporated chitosan/gelatin composite for the sequestration of chromium(VI) and fluoride from water. Chemosphere 262:128317
37. Muthu Prabhu S, Elanchezhiyan SS, Lee G, Meenakshi S (2016) Defluoridation of water by *Tea-bag* model using $La^{3+}$ modified synthetic resin@chitosan biocomposite. Int J Biol Macromol 91:1002–1009
38. Muthu Prabhu S, Subaramanian M, Meenakshi S (2016) A simple one-pot in-situ method for the synthesis of aluminum and lanthanum binary oxyhydroxides in chitosan template towards defluoridation of water. Chem Eng J 283:1081–1089
39. Chaudhary M, Rawat S, Jain N, Bhatnagar A, Maiti A (2019) Chitosan-Fe-Al-Mn metal oxyhydroxides composite as highly efficient fluoride scavenger for aqueous medium. Carbohydr Polym 216:140–148
40. Srivastava A, Kumari M, Ramanathan A, Selvaraj K et al (2020) Removal of fluoride from aqueous solution by mesoporous silica nanoparticles functionalized with chitosan derived from mushroom. J Macromol Sci A 57:619–627
41. Zhu T, Zhu T, Gao J, Zhang L, Zhang W (2017) Enhanced adsorption of fluoride by cerium immobilized cross-linked chitosan composite. J Fluor Chem 194:80–88
42. Hao L, Liu M, Wang N, Li G (2018) A critical review on arsenic removal from water using iron-based adsorbents. RSC Adv 8:39545–39560
43. Kwok KCM, Koong LF, Chen G, McKay G (2014) Mechanism of arsenic removal using chitosan and nanochitosan. J Colloid Interface Sci 416:1–10

44. Chen CC, Chung YC (2006) Arsenic removal using a biopolymer chitosan sorbent. J Environ Sci Health A Tox Hazard Subst Environ Eng 41:645–658
45. Pontoni L, Fabbricino M (2012) Use of chitosan and chitosan-derivatives to remove arsenic from aqueous solutions – a mini review. Carbohydr Res 356:86–92
46. Lin X, Wang L, Jiang S, Cui L, Wu G (2019) Iron-doped chitosan microsphere for As(III) adsorption in aqueous solution: kinetic, isotherm and thermodynamic studies. Korean J Chem Eng 36:1102–1114
47. Priya VN, Rajkumar M, Magesh G, Mobika J, Sibi SPL (2020) Chitosan assisted Fe-Al double layered hydroxide/reduced graphene oxide composites for As(V) removal. Mater Chem Phys 251
48. Shan H, Peng S, Zhao C, Zhan H, Zeng C (2020) Highly efficient removal of As(III) from aqueous solutions using goethite/graphene oxide/chitosan nanocomposite. Int J Biol Macromol 164:13–26
49. Abou El-Reash YG, Otto M, Kenawy IM, Ouf AM (2011) Adsorption of Cr(VI) and As (V) ions by modified magnetic chitosan chelating resin. Int J Biol Macromol 49:513–522
50. Liu B, Wang D, Li H, Xu Y, Zhang L (2011) As(III) removal from aqueous solution using $\alpha$-$Fe_2O_3$ impregnated chitosan beads with As(III) as imprinted ions. Desalination 272:286–292
51. Chauhan D, Dwivedi J, Sankararamakrishnan N (2014) Novel chitosan/PVA/zerovalent iron biopolymeric nanofibers with enhanced arsenic removal applications. Environ Sci Pollut Res Int 21:9430–9442
52. Wang J, Xu W, Chen L, Huang X, Liu J (2014) Preparation and evaluation of magnetic nanoparticles impregnated chitosan beads for arsenic removal from water. Chem Eng J 251:25–34
53. Ren L, Zhou W, Sun B, Li H et al (2019) Defects-engineering of magnetic γ-Fe2O3 ultrathin nanosheets/mesoporous black TiO2 hollow sphere heterojunctions for efficient charge separation and the solar-driven photocatalytic mechanism of tetracycline degradation. Appl Catal Environ 240:319–328
54. Salih SS, Mahdi A, Kadhom M, Ghosh TK (2019) Competitive adsorption of As(III) and As (V) onto chitosan/diatomaceous earth adsorbent. J Environ Chem Eng 7
55. Zhang S, Liu Y, Gu P, Ma R et al (2019) Enhanced photodegradation of toxic organic pollutants using dual-oxygen-doped porous g-C3N4: mechanism exploration from both experimental and DFT studies. Appl Catal Environ 248:1–10
56. Ayub A, Raza ZA, Majeed MI, Tariq MR, Irfan A (2020) Development of sustainable magnetic chitosan biosorbent beads for kinetic remediation of arsenic contaminated water. Int J Biol Macromol 163:603–617
57. de Brião, G. V., de Andrade, J. R., da Silva, M. G. C., Vieira, M. G. A., Removal of toxic metals from water using chitosan-based magnetic adsorbents. A review. Environ Chem Lett 2020, 18, 1145–1168
58. Kloster GA, Valiente M, Marcovich NE, Mosiewicki MA (2020) Adsorption of arsenic onto films based on chitosan and chitosan/nano-iron oxide. Int J Biol Macromol 165:1286–1295
59. Lobo C, Castellari J, Colman Lerner J, Bertola N, Zaritzky N (2020) Functional iron chitosan microspheres synthesized by ionotropic gelation for the removal of arsenic (V) from water. Int J Biol Macromol 164:1575–1583
60. Sierra-Trejo PV, Guibal E, Louvier-Hernández JF (2020) Arsenic sorption on chitosan-based sorbents: comparison of the effect of molybdate and tungstate loading on As(V) sorption properties. J Polym Environ 28:934–947
61. Tan P, Zheng Y, Hu Y (2020) Efficient removal of arsenate from water by lanthanum immobilized electrospun chitosan nanofiber. Colloids Surf A Physicochem Eng Asp 589
62. Yang Q, Gong L, Huang L, Xie Q et al (2020) Adsorption of As(V) from aqueous solution on chitosan-modified diatomite. Int J Environ Res Public Health 17

63. Zeng H, Wang F, Xu K, Zhang J, Li D (2020). Optimization and regeneration of chitosan-alginate hybrid adsorbent embedding iron-manganese sludge for arsenic removal. Colloids Surf A 607:125500
64. Zeng H, Yu Y, Wang F, Zhang J, Li D (2020) Arsenic(V) removal by granular adsorbents made from water treatment residuals materials and chitosan. Colloids Surf A Physicochem Eng Asp 585
65. Zeng J, Qi P, Shi J, Pichler T et al (2020) Chitosan functionalized iron nanosheet for enhanced removal of As(III) and Sb(III): synergistic effect and mechanism. Chem Eng J 382
66. Muthu Prabhu S, Sasaki K (2017) Fabrication of chitosan-reinforced $Zr_xAl_{1-x}OOH$ nanocomposites and their arsenite and fluoride depollution densities from single/binary systems. ChemistrySelect 2:6375–6387
67. Hamoudi S, Belkacemi K (2013) Adsorption of nitrate and phosphate ions from aqueous solutions using organically-functionalized silica materials: kinetic modeling. Fuel 110:107–113
68. Mohsen MS (2004) Treatment and reuse of industrial effluents: case study of a thermal power plant. Desalination 167:75–86
69. Kumar IA, Jeyaprabha C, Meenakshi S, Viswanathan N (2019) Hydrothermal encapsulation of lanthanum oxide derived *Aegle marmelos* admixed chitosan bead system for nitrate and phosphate retention. Int J Biol Macromol 130:527–535
70. Kumar IA, Jeyaprabha C, Viswanathan N (2020) Effect of polyvalent metal ions encrusted biopolymeric hybrid beads on nitrate adsorption. J Environ Chem Eng 8:103894
71. Banu HT, Karthikeyan P, Meenakshi S (2019) $Zr^{4+}$ ions embedded chitosan-soya bean husk activated bio-char composite beads for the recovery of nitrate and phosphate ions from aqueous solution. Int J Biol Macromol 130:573–583
72. Jiang H, Chen P, Luo S, Tu X et al (2013) Synthesis of novel nanocomposite $Fe_3O_4/ZrO_2$/chitosan and its application for removal of nitrate and phosphate. Appl Surf Sci 284:942–949
73. Karthikeyan P, Banu HAT, Meenakshi S (2019) Removal of phosphate and nitrate ions from aqueous solution using $La^{3+}$ incorporated chitosan biopolymeric matrix membrane. Int J Biol Macromol 124:492–504
74. Karthikeyan P, Banu HAT, Meenakshi S (2019) Synthesis and characterization of metal loaded chitosan-alginate biopolymeric hybrid beads for the efficient removal of phosphate and nitrate ions from aqueous solution. Int J Biol Macromol 130:407–418
75. Karthikeyan P, Meenakshi S (2019) In-situ fabrication of cerium incorporated chitosan-β-cyclodextrin microspheres as an effective adsorbent for toxic anions removal. Environ Nanotechnol Monitor Manage 12:100272
76. Karthikeyan P, Meenakshi S (2019) In-situ fabrication of zirconium entrenched biopolymeric hybrid membrane for the removal of toxic anions from aqueous medium. Int J Biol Macromol 141:1199–1209
77. Karthikeyan P, Vigneshwaran S, Meenakshi S (2020) Al3+ incorporated chitosan-gelatin hybrid microspheres and their use for toxic ions removal: assessment of its sustainability metrics. Environ Chem Ecotoxicol 2:97–106
78. Kim J-H, Kim S-B, Lee S-H, Choi J-W (2018) Laboratory and pilot-scale field experiments for application of iron oxide nanoparticle-loaded chitosan composites to phosphate removal from natural water. Environ Technol 39:770–779
79. Kumar IA, Viswanathan N (2017) Development of multivalent metal ions imprinted chitosan biocomposites for phosphate sorption. Int J Biol Macromol 104:1539–1547
80. Liu Q, Hu P, Wang J, Zhang L, Huang R (2016) Phosphate adsorption from aqueous solutions by zirconium (IV) loaded cross-linked chitosan particles. J Taiwan Inst Chem Eng 59:311–319
81. Liu X, Zhang L (2015) Removal of phosphate anions using the modified chitosan beads: adsorption kinetic, isotherm and mechanism studies. Powder Technol 277:112–119
82. Mahaninia MH, Wilson LD (2016) Cross-linked chitosan beads for phosphate removal from aqueous solution. J Appl Polym Sci 133

83. Nthumbi RM, Catherine Ngila J, Moodley B, Kindness A, Petrik L (2012) Application of chitosan/polyacrylamide nanofibres for removal of chromate and phosphate in water. Phys Chem Earth 50–52:243–251
84. Sowmya A, Meenakshi S (2013) An efficient and regenerable quaternary amine modified chitosan beads for the removal of nitrate and phosphate anions. J Environ Chem Eng 1:906–915
85. Sowmya A, Meenakshi S (2014) A novel quaternized chitosan–melamine–glutaraldehyde resin for the removal of nitrate and phosphate anions. Int J Biol Macromol 64:224–232
86. Sowmya A, Meenakshi S (2014) Effective removal of nitrate and phosphate anions from aqueous solutions using functionalised chitosan beads. Desalin Water Treat 52:2583–2593
87. Sowmya A, Meenakshi S (2015) Phosphate uptake studies on different types of lanthanum-loaded polymeric materials. Environ Prog Sustain Energy 34:146–154
88. Sowmya A, Meenakshi S (2014) Zr(IV) loaded cross-linked chitosan beads with enhanced surface area for the removal of nitrate and phosphate. Int J Biol Macromol 69:336–343
89. Sowmya A, Meenakshi S (1674-1683) Effective utilization of the functional groups in chitosan by loading Zn(II) for the removal of nitrate and phosphate. Desalin Water Treat 2015:54
90. Thagira Banu H, Karthikeyan P, Meenakshi S (2018) Lanthanum (III) encapsulated chitosan-montmorillonite composite for the adsorptive removal of phosphate ions from aqueous solution. Int J Biol Macromol 112:284–293
91. Zavareh S, Behrouzi Z, Avanes A (2017) Cu (II) binded chitosan/$Fe_3O_4$ nanocomomposite as a new biosorbent for efficient and selective removal of phosphate. Int J Biol Macromol 101:40–50
92. Kumar IA, Viswanathan N (2018) Preparation and testing of a tetra-amine copper(II) chitosan bead system for enhanced phosphate remediation. Carbohydr Polym 183:173–182
93. Kumar IA, Viswanathan N (2019) Hydrothermal fabrication of amine-grafted magnetic gelatin hybrid composite for effective adsorption of nitrate and phosphate. Ind Eng Chem Res 58:21521–21530
94. Kumar IA, Viswanathan N (2018) Hydrothermal fabrication of zirconium oxyhydroxide capped chitosan/kaolin framework for highly selective nitrate and phosphate retention. Ind Eng Chem Res 57:14470–14481
95. Kumar IA, Viswanathan N (2019) Development of magnetic particles encrusted LDH-admixed biopolymeric complex beads for selective phosphate remediation. J Chem Eng Data 64:5725–5736
96. Zhao T, Feng T (2016) Application of modified chitosan microspheres for nitrate and phosphate adsorption from aqueous solution. RSC Adv 6:90878–90886
97. Golie WM, Upadhyayula S (2017) An investigation on biosorption of nitrate from water by chitosan based organic-inorganic hybrid biocomposites. Int J Biol Macromol 97:489–502
98. Banu HT, Meenakshi S (2017) One pot synthesis of chitosan grafted quaternized resin for the removal of nitrate and phosphate from aqueous solution. Int J Biol Macromol 104:1517–1527
99. Hu Q, Chen N, Feng C, Hu W (2015) Nitrate adsorption from aqueous solution using granular chitosan-$Fe^{3+}$ complex. Appl Surf Sci 347:1–9
100. Zhang B, Chen N, Feng C, Zhang Z (2018) Adsorption for phosphate by crosslinked/non-crosslinked-chitosan-Fe(III) complex sorbents: characteristic and mechanism. Chem Eng J 353:361–372
101. Zhao Y, Guo L, Shen W, An Q et al (2020) Function integrated chitosan-based beads with throughout sorption sites and inherent diffusion network for efficient phosphate removal. Carbohydr Polym 230:115639
102. Teimouri A, Nasab SG, Vahdatpoor N, Habibollahi S et al (2016) Chitosan/zeolite Y/Nano $ZrO_2$ nanocomposite as an adsorbent for the removal of nitrate from the aqueous solution. Int J Biol Macromol 93:254–266

103. Salehi S, Hosseinifard M (2020) Optimized removal of phosphate and nitrate from aqueous media using zirconium functionalized nanochitosan-graphene oxide composite. Cellul 27:8859–8883
104. Yazdani MR, Virolainen E, Conley K, Vahala R (2018) Chitosan–zinc(II) complexes as a bio-sorbent for the adsorptive abatement of phosphate: mechanism of complexation and assessment of adsorption performance. Polymers 10:25
105. Yazdi F, Anbia M, Salehi S (2019) Characterization of functionalized chitosan-clinoptilolite nanocomposites for nitrate removal from aqueous media. Int J Biol Macromol 130:545–555
106. Fu C-C, Tran HN, Chen X-H, Juang R-S (2020) Preparation of polyaminated $Fe_3O_4$@chitosan core-shell magnetic nanoparticles for efficient adsorption of phosphate in aqueous solutions. J Ind Eng Chem 83:235–246
107. Liu B, Yu Y, Han Q, Lou S et al (2020) Fast and efficient phosphate removal on lanthanum-chitosan composite synthesized by controlling the amount of cross-linking agent. Int J Biol Macromol 157:247–258